GEOPHYSICAL RESEARCH LETTERS, VOL. 40, 1–5, doi:10.1002/2013GL058087, 2013

Typhoon-induced concentric airglow structures in the mesopause region

S. Suzuki,[1] S. L. Vadas,[2] K. Shiokawa,[1] Y. Otsuka,[1] S. Kawamura,[3] and Y. Murayama[3]

Received 20 September 2013; revised 24 October 2013; accepted 28 October 2013.

[1] We present the first reported gravity wave patterns in the mesopause region caused by a typhoon in the troposphere. On 10 December 2002, concentric rings of gravity waves in OH airglow were observed simultaneously by all-sky imagers in the Optical Mesosphere and Thermosphere Imager system in Japan, located at Rikubetsu (43.5°N, 143.8°E), Shigaraki (34.9°N, 136.1°E), and Sata (31.0°N, 130.7°E). The airglow structures, which were well defined and formed a coherent wave pattern expanding concentrically, were identified over 8 h (2135–2947 LT). We estimate the horizontal wavelength, horizontal phase speed, and wave period as 34.5 km, 50.2 m s^{-1}, and 11.5 min, respectively. Infrared cloud images from the Geostationary Meteorological Satellite show that the center of the rings estimated from the airglow data corresponds to a spiral band of Typhoon Pongsona (T0226). This unique event provides new insight into coupling between the lower and upper atmosphere.
Citation: Suzuki, S., S. L. Vadas, K. Shiokawa, Y. Otsuka, S. Kawamura, and Y. Murayama (2013), Typhoon-induced concentric airglow structures in the mesopause region, *Geophys. Res. Lett.*, *40*, doi:10.1002/2013GL058087.

1. Introduction

[2] Gravity waves propagating in the mesosphere and lower thermosphere (MLT) provide important information on dynamic coupling between the lower and upper atmosphere. They can also explain how meteorological disturbances affect dynamics in the region ∼100 km above the ground and how they influence global circulation. Energy and momentum are transported into the upper atmosphere by gravity waves generated in the lower atmosphere, and these play important roles in the wind and thermal balances in the MLT region; particularly, short-period (< 1 h) and small-scale (< 100 km) waves contribute to the dynamics as a consequence of their significant momentum flux [*Fritts and Vincent*, 1987; *Nastrom and Fritts*, 1992].

[3] Airglow imaging is an especially useful technique for observing such small-scale gravity waves in the MLT. Observations with airglow imagers can reveal the two-dimensional (2-D) horizontal features of the waves with high temporal and spatial resolutions. Many studies have used airglow imagers to report the statistics of MLT gravity waves around the world, thus revealing a global view of gravity wave activities [*Suzuki et al.*, 2009a, and references therein].

[4] Based on the 2-D structure of the gravity waves observed in airglow, several studies have also used reverse ray-tracing techniques to deduce sources for these waves in the lower atmosphere [e.g., *Wrasse et al.*, 2006; *Suzuki et al.*, 2013a]. Concentric rings, which very occasionally appear in airglow images, provide a more intuitive one-to-one correspondence between a meteorological source and a wave in the MLT. Localized strong convection can overshoot the tropopause and radiate gravity waves with a conically shaped phase surface.

[5] Numerical simulations have produced similar concentric patterns in gravity waves [*Horinouchi et al.*, 2002; *Alexander et al.*, 2004; *Vadas et al.*, 2009]. There have been nearly a dozen observations of such patterns in airglow [*Taylor and Hapgood*, 1988; *Suzuki et al.*, 2007a; *Yue et al.*, 2009; *Vadas et al.*, 2012]. *Suzuki et al.* [2007a] suggested that successfully measuring concentric rings in the airglow heights requires a sufficiently weak wind field to maintain their vertical propagation and coherency to the MLT region. *Vadas et al.* [2012] demonstrated that mesospheric concentric gravity waves generated by multiple storms simulated using the background model wind agree well with the observations by *Yue et al.* [2009]. Although observations have been limited, concentric gravity wave rings provide valuable information on atmospheric coupling between the lower and upper atmosphere.

[6] Thus far, no observational evidence for that waves induced by extreme cyclones (such as typhoon, hurricane, and tropical cyclone) reaching the mesopause region has been reported, despite the fact that such a cyclone contains extremely intense regions of convection that actively excite waves upward. Poor weather conditions over a wide area associated with the anvil cloud of an approaching strong cyclone is one reason for the lack of evidence, since as far as ground-based optical measurements are concerned, a cloudless sky is essential for accurate observation.

[7] In this paper, we report on a concentric wave event observed on 10 December 2002, for which the data strongly suggests that the wave was generated from Typhoon Pongsona and that it propagated up to the height of airglow layer near the mesopause.

2. Observations and Analysis

[8] The Solar-Terrestrial Environment Laboratory, Nagoya University, has conducted airglow-imaging observations with all-sky airglow imagers using the Optical

Additional supporting information may be found in the online version of this article.

[1]Solar-Terrestrial Environment Laboratory, Nagoya University, Nagoya, Japan.
[2]NorthWest Research Associates, Inc., Boulder, Colorado, USA.
[3]National Institute of Information and Communications Technology, Koganei, Japan.

Corresponding author: S. Suzuki, Solar-Terrestrial Environment Laboratory, Nagoya University, Furo-cho, Chikusa-ku, Nagoya 464-8601, Japan. (shin@stelab.nagoya-u.ac.jp)

©2013. American Geophysical Union. All Rights Reserved.
0094-8276/13/10.1002/2013GL058087

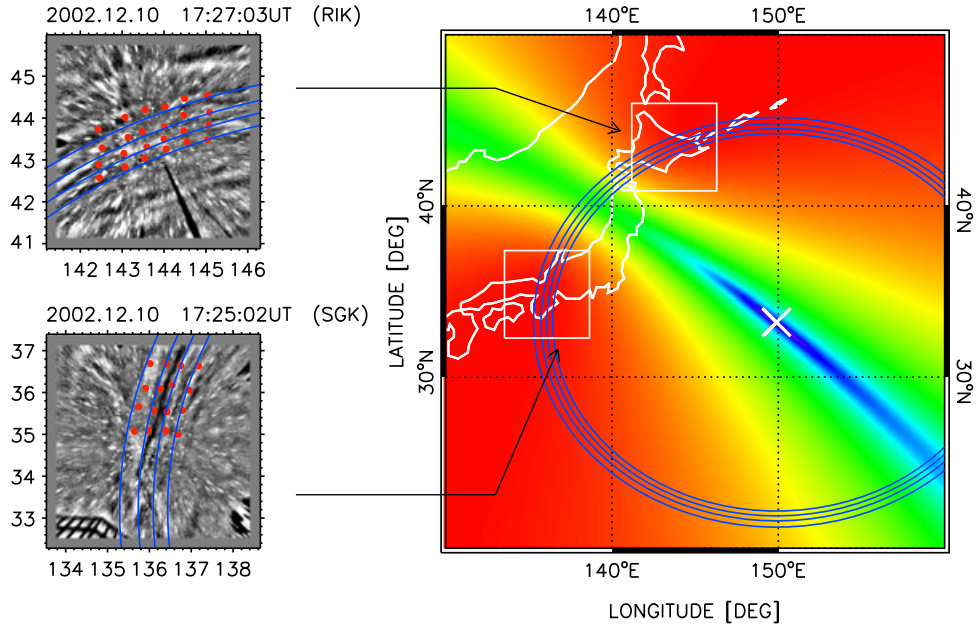

Figure 1. (left) Airglow images taken over RIK at 1727 UT and SGK at 1725 UT. The red dots represent traces of bright wavefronts in the airglow. (right) A contour map showing the total residual sum of squares between the observed and computed wavefronts, calculated by changing the center of the concentric circles. Bluish and reddish colors indicate smaller and larger values, respectively. The blue circles show structures calculated to fit the airglow data with the center marked by a cross, at which the contour value is at a minimum.

Mesosphere and Thermosphere Imager (OMTI) system [*Shiokawa et al.*, 2009]. Very recently, *Suzuki et al.* [2013b] developed an analysis environment for simultaneous airglow imaging network data from multipoint observations by the OMTI system, which enables us to detect airglow structures in the MLT with a spatial extent covering all of Japan.

[9] Based on the network analysis, we found expanding rings of a concentric gravity wave in the OH Mienel emission images (wavelength: 720–910 nm, emission height: ~85 km) on 10 December 2002. In this event, three imagers were in operation at three Japanese stations: Rikubetsu (RIK: 43.5°N, 143.8°E), Shigaraki (SGK: 34.9°N, 136.1°E), and Sata (STA: 31.0°N, 130.7°E). The OH airglow measurements at all stations were performed with an image acquisition cycle of 5.5 min and an exposure time of 15 s. Animation S1 in the supporting information shows the expanding rings in the multistation OH airglow images, depicted as time-difference intensities (TDI) projected onto geographical coordinates, with sizes of ~500 km × ~500 km, by assuming an emission height of 85 km. Concentric arcs extending over the three stations can be recognized for ~ 8 h in the period 1240–2047 UT (2140–2947 LT). Unfortunately, most images taken at STA (the southernmost station) were rendered unusable due an overcast sky. However, wave structures seen through wisps of cloud in the north part of the field of view that were visible over 1655–1730 UT were consistent with the arcs observed at RIK and SGK; the wave was elongated in the meridional direction and moved westward at STA.

[10] We can estimate the entire wave structure from the fragments of the arc observed at RIK and SGK by assuming that the wave has circular wavefronts expanding concentrically from a point. First, we trace successive wavefronts in the airglow images taken at RIK and SGK, with the intensity of the airglow enhanced, as shown in Figure 1 (left). We note that the airglow images in Figure 1 are not TDIs but rather filtered images with a median size of 100 km × 100 km. This is in order to depict the locations of the wavefronts accurately; the TDIs cause substantial shifts in the wave structure depending on the sampling times of airglow images as well as their wave parameters. Second, we fit concentric circles to the observations (the traced points) by a least squares method by modifying the center position. The best fit set of circles is produced when the total residual sum of squares S is minimized [*Hapgood and Taylor*, 1982]:

$$S = \sum_k \left[\sum_i (r_{ik} - r_k)^2 \right], \quad (1)$$

where r_{ik} is the distance from an assumed center at latitude λ_c and longitude ϕ_c to the ith traced point on the kth wavefront (λ_{ik}, ϕ_{ik}), and $r_k = \sum_i r_{ik}/N_k$ is the mean radius of the kth wavefront, where N_k is the number of points on the kth wavefront. According to spherical trigonometry, r_{ik} can be written as

$$r_{ik} = R_e \cos^{-1} \left[\sin\phi_c \sin\phi_{ik} + \cos\phi_c \cos\phi_{ik} \cos(\lambda_{ik} - \lambda_c) \right], \quad (2)$$

where R_e is the radius of the Earth.

[11] The distribution of the S value computed within a range of ϕ_c=130°E–160°E and λ_c=20°N–50°N is shown in Figure 1 (right). The white cross and blue circles represent the center and computed wavefronts with the minimum value of S, respectively. The computed center is located at (33.2°N, 149.9°E) approximately 1200 km away from Japan. It is worth noting here that it is difficult to determine directly which wavefronts actually connect between the images at RIK and SGK due to the observational gap between their field of views. The correspondence of the four wavefronts in the abovementioned analysis is derived by using all combinations of pairs to minimize S in equation (1).

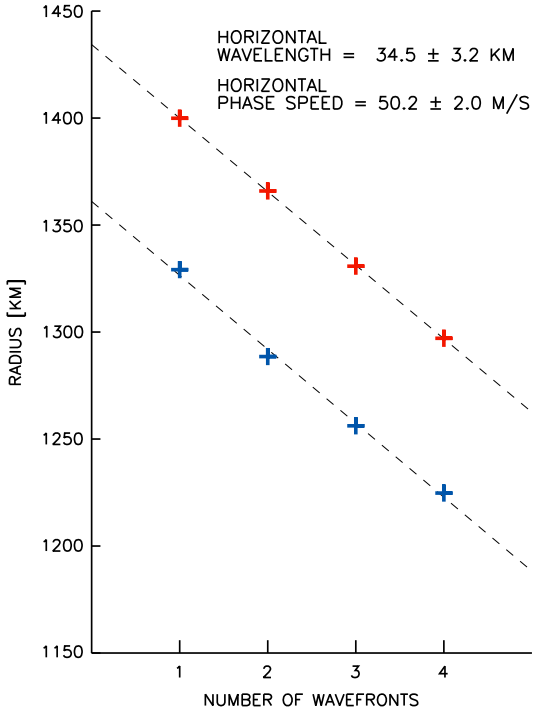

Figure 2. Estimation of wave parameters from the calculated rings. The crosses indicate the radii of the best fitting set of wavefronts; blue set is the rings shown in Figure 1 (RIK at 1727 UT and SGK at 1725 UT) and the red set is calculated using airglow images after 24.5 min (RIK at 1751 UT and SGK at 1749 UT). The dashed lines indicate the regression lines of the two sets.

[12] Figure 2 depicts the estimated wave parameters of the concentric gravity waves. The set of blue crosses represents the radii of the circles calculated to fit the data, shown in Figure 1, numbered from the outer to the inner ring. The set of red crosses is derived from airglow images obtained after 24.5 min in a similar manner, but adjusted to have a common center as estimated above (33.2°N, 149.9°E). The horizontal wavelength is estimated by averaging the differences between each ring radius and found to be 34.5 km. The horizontal phase speed is estimated from how far each structure has traveled in the 24.5 min (i.e., from the red set to the blue set) and was found to be 50.2 m s^{-1}. Figure 2 shows a linear regression at both times; their gradients are comparable to each other. These parameters yield a wave period of 11.5 min. It is also worth noting that the airglow images at the OMTI stations were not taken simultaneously, such that their sampling times are slightly different; for example, as shown in Figure 1, the images at RIK and SGK were obtained at 1727 and 1725 UT, respectively. This time lag (2 min) caused the wavefronts to shift by ~6 km between the images at the two stations.

[13] Finally, we roughly estimate how much momentum could be carried upward by the observed gravity wave using the procedure described by *Suzuki et al.* [2010], who adopted the cancellation factor model [*Vargas et al.*, 2007]. For the intrinsic parameters of the observed wave in the calculation of momentum flux, we use background winds obtained by the MF radars over Wakkanai (45.4°N, 141.7°E) and Yamagawa (31.2°N, 130.6°E). The averaged wind over the two stations was directed eastward (101.6° clockwise from north) at 13.2 m s^{-1} in the OH airglow height during the event interval. With an airglow intensity variation of ~2.5%, the momentum flux is estimated to be 3.0–5.1 m^2 s^{-2}, which varies with direction (i.e., the intrinsic parameters). These values are only slightly larger than the estimates made from a concentric gravity wave observed in OH airglow over SGK and generated from a thunderstorm, which had a momentum flux of 2.2 m^2 s^{-2} [*Suzuki et al.*, 2007a]. These values are comparable with the small-scale gravity waves commonly seen in airglow measurements, the majority of which have a flux less than 10 m^2 s^{-2} [*Suzuki et al.*, 2007b, 2009b; *Tang et al.*, 2005]. However, the long-lasting and spatially widespread pattern in the present event can contribute much more to dynamics in the upper atmosphere.

3. Discussion

[14] Previous studies on concentric gravity waves in the mesospheric airglow have found the sources to be strong tropospheric convection from thunderstorms at the centers of the structures [*Taylor and Hapgood*, 1988; *Sentman et al.*, 2003; *Suzuki et al.*, 2007a; *Vadas et al.*, 2009, 2012; *Yue et al.*, 2009]. In our case, the most likely source is convection within a powerful typhoon, Typhoon Pongsona (T0226), which traveled over the Pacific Ocean in the southeast of Japan.

[15] Figure 3 shows the track of Typhoon Pongsona for 10 days from 2 December 2002. The typhoon evolved while proceeding northwestward, reaching a mature stage with a

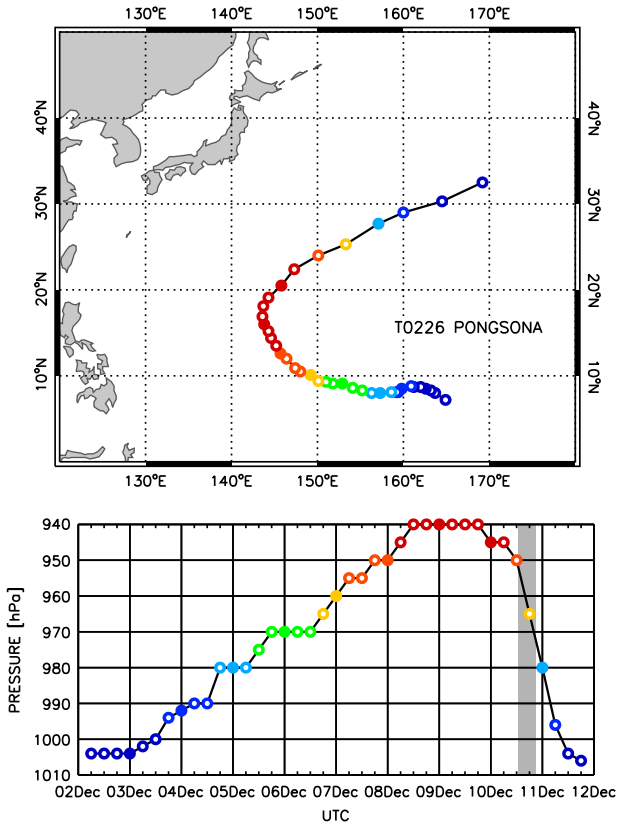

Figure 3. The track of Typhoon Pongsona from 2 to 11 December 2002 every 6 hours; the filled circles represent points at 0000 UT. The colors denote the central pressure as shown in the bottom plot.

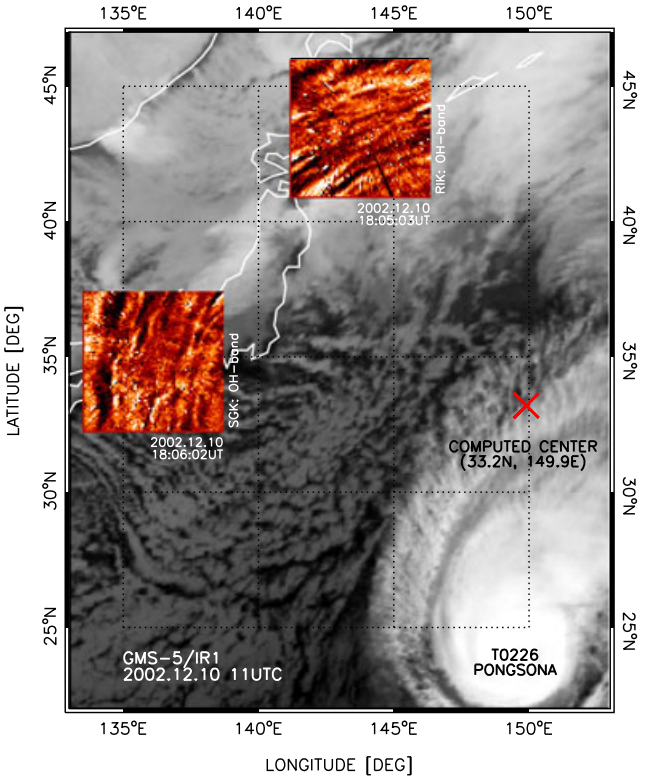

Figure 4. A combined map of the observed concentric airglow structure over RIK at 1805 UT and SGK at 1806 UT overlaid on the GMS-5 IR cloud image at 1132 UT. The red cross indicates the location of the computed center of the concentric rings.

central pressure of 940 hPa and peak winds of ∼45 m s^{-1}. After 9 December, Typhoon Pongsona changed its path northeastward and began to weaken swiftly. The center of Typhoon Pongsona was closest to Japan on 10 December; we note that the concentric rings in the airglow were also observed on the night of 10 December, in which the typhoon was in its ebb stage, as shown by a gray-shaded interval in Figure 3.

[16] Figure 4 shows a combined map of the airglow observations overlaid on the infrared (IR) (10.5–11.5 μm) cloud image obtained by the Geostationary Meteorological Satellite 5 (GMS-5) at 1132 UT. Animation S2 summarizes the airglow observations made in this paper in the same format as Figure 4. The airglow images lag over 6 hours behind the satellite IR data, considering the propagation time from the center of the rings (their source location) to Japan. The IR cloud image shows that the computed center is located in the spiral band (the arm of the typhoon), which is ∼1000 km away from the center of the typhoon. In the spiral band, many localized high clouds develop [*Sato*, 1993], and hence, gravity waves can be actively generated there. Thus, the concentric gravity wave observed in the OH airglow in this study is likely to have originated from the spiral band of Typhoon Pongsona.

[17] Based on a numerical model, *Vadas et al.* [2009] investigated the effects of background wind on concentric wave structures excited from a convective plume. They found that a strong wind field in the middle atmosphere could shift the apparent centers of concentric rings at the mesopause height and also block the propagation of concentric rings anisotropically, causing "squashed" ring patterns. Thus, for the estimation of wave structure performed in the previous section, it may have been better to fit ellipses (rather than circles) to deduce more realistic wavefronts. Fitting of ellipses, however, involves high uncertainties and is impractical, since the airglow observations covered only a portion of the entire concentric structure. Besides, fitting with circles caused no significant discrepancy between the calculated circlar phase lines and the observed phase structure of the wave (see Figure 1).

[18] These results may imply that wind fields in the middle atmosphere were weak enough to not squash the wave structure and shift the center to the wave source at the airglow height, even though there is typically a strong eastward wind in the lower mesosphere in the midlatitudes during winter. Such calm wind conditions have also been suggested for previous observations of concentric gravity waves, which had nearly perfectly circular airglow structures [*Suzuki et al.*, 2007a; *Yue et al.*, 2009]. This implies that the stratospheric and mesospheric winds must have been relatively small.

[19] *Vadas et al.* [2009] also found an interesting feature of the concentric gravity waves that modeled horizontal wavelengths increase with radius. Such a tendency can be slightly seen in Figure 2; the inner structures have smaller horizontal wavelengths than the outer structures. However, almost uniform wavelengths regardless of radius still best explains Figure 2. Note that the range in radius here, however, is small in comparison with *Vadas et al.* [2009], which included all of the concentric gravity wave (including the center).

[20] Gravity waves induced by typhoons reaching the mesopause have not been reported. On the other hand, there have been several observational and numerical studies of those in the stratosphere [*Kuester et al.*, 2008; *Kim et al.*, 2009; *Chane Ming et al.*, 2010]. *Kim et al.* [2009] demonstrated stratospheric gravity waves generated by Typhoon Ewiniar, by using numerical simulations as well as the European Center for Medium-Range Weather Forecasts (ECMWF) analysis data and the Atmospheric Infrared Sounder (AIRS) measurements from space. The simulation showed that typhoon-induced arc-like gravity waves propagated from the typhoon into the stratosphere (up to 42 km); the wave characteristics were in good agreement with the ECMWF data and AIRS measurements. The horizontal scale of the waves, at a few hundred kilometers, is greater than that in the presented paper. However, as the authors pointed out, the results of their numerical simulations were highly dependent on the model resolution and there remained uncertainties for smaller-scale waves.

[21] Based on a model study of gravity waves generated by convection within a tropical cyclone, *Kuester et al.* [2008] showed that large-amplitude waves with a horizontal wavelength of ∼30 km in the lower stratosphere. Although further investigations are needed, comparisons between the stratospheric and mesospheric wave structures give an insight into vertical propagation of gravity waves emanating from an extreme cyclone from the lower to the upper atmosphere. Our study offers, for the first time, a response in the mesopause region, which is spatially widespread airglow patterns, to a typhoon may suggest that such a strong

convection could affect the ionospheric dynamics in regions far away from the origin.

4. Conclusions

[22] We reported on a concentric gravity wave observed in the mesospheric airglow with a multistation network in Japan on 10 December 2002. We estimated that the wave had a horizontal wavelength of 34.5 km and that it expanded concentrically at a phase speed of 50.2 m s^{-1} with a wave period of 11.5 min. The airglow pattern appeared for ∼8 h (the entire period of the airglow observations). We estimated the momentum flux to be 3.0–5.1 m^2 s^{-2}. We believe this wave was generated by convection within Typhoon Pongsona, which was located around the center of the observed airglow rings at the time of observation.

[23] This event displayed a concentric pattern with larger radii than found in previous airglow measurements. It is easy to imagine that the scale reflects the spatial size of the wave source and distance traveled from the troposphere to the mesosphere. A single airglow imager is limited in the spatial extent it can cover. Therefore, observations with a multistation imaging network are quite useful in monitoring atmospheric coupling between the lower and upper atmosphere in greater detail, as this paper has evidenced.

[24] **Acknowledgments.** GMS-5 cloud data used in this study were provided by CEReS, Chiba University. This work was supported by the Grants-in-Aid for Scientific Research (18403011, 20244080, and 23740368) from the MEXT, Japan, and the joint research program of STEL, Nagoya University. Research support for SS is provided by the YLC program of IAR, Nagoya University. SLV was supported by NSF grant AGS-1139149.

[25] The Editor thanks two anonymous reviewers for their assistance in evaluating this paper.

References

Alexander, M. J., P. T. May, and J. H. Beres (2004), Gravity waves generated by convection in the Darwin area during the Darwin Area Wave Experiment, *J. Geophys. Res.*, *109*, D20S04, doi:10.1029/2004JD004729.

Chane Ming, F., Z. Chen, and F. Roux (2010), Analysis of gravity-waves produced by intense tropical cyclones, *Ann. Geophys.*, *28*, 531–547.

Fritts, D. C., and R. A. Vincent (1987), Mesospheric momentum flux studies at Adelaide, Australia: Observations and a gravity wave-tidal interaction model, *J. Atmos. Sci.*, *44*, 605–619.

Hapgood, M. A., and M. J. Taylor (1982), Analysis of airglow image data, *Ann. Geophys.*, *38*, 805–813.

Horinouchi, T., T. Nakamura, and J.-i. Kosaka (2002), Convectively generated mesoscale gravity waves simulated throughout the middle atmosphere, *Geophys. Res. Lett.*, *29*(21), 2007, doi:10.1029/2002GL016069.

Kim, S.-Y., H.-Y. Chun, and D. L. Wu (2009), A study on stratospheric gravity waves generated by Typhoon Ewiniar: Numerical simulations and satellite observations, *J. Geophys. Res.*, *114*, D22104, doi:10.1029/2009JD011971.

Kuester, M. A., M. J. Alexander, and E. A. Ray (2008), A model study of gravity waves over Hurricane Humberto (2001), *J. Atmos. Sci.*, *65*, 3231–3246.

Nastrom, G. D., and D. C. Fritts (1992), Sources of mesoscale variability of gravity waves, I: Topographic excitation, *J. Atmos. Sci.*, *49*, 101–110.

Sato, K. (1993), Small-scale wind disturbances observed by the MU radar during the passage of Typhoon Kelly, *J. Atmos. Sci.*, *50*, 518–537.

Sentman, D. D., E. M. Wescott, R. H. Picard, J. R. Winick, H. C. Stenbaek-Nielsen, E. M. Dewan, D. R. Moudry, F. T. São Sabbas, M. J. Heavner, and J. Morrill (2003), Simultaneous observations of mesospheric gravity waves and sprites generated by a midwestern thunderstorm, *J. Atmos. Terr. Phys.*, *65*, 537–550.

Shiokawa, K., Y. Otsuka, and T. Ogawa (2009), Propagation characteristics of nighttime mesospheric and thermospheric waves observed by optical mesosphere thermosphere imagers at middle and low latitudes, *Earth Planets Space*, *61*, 479–491.

Suzuki, S., K. Shiokawa, Y. Otsuka, T. Ogawa, K. Nakamura, and T. Nakamura (2007a), A concentric gravity wave structure in the mesospheric airglow images, *J. Geophys. Res.*, *112*, D02102, doi:10.1029/2005JD006558.

Suzuki, S., K. Shiokawa, Y. Otsuka, T. Ogawa, M. Kubota, M. Tsutsumi, T. Nakamura, and D. C. Fritts (2007b), Gravity wave momentum flux in the upper mesosphere derived from OH airglow imaging measurements, *Earth Planets Space*, *59*, 421–428.

Suzuki, S., K. Shiokawa, K. Hosokawa, K. Nakamura, and W. K. Hocking (2009a), Statistical characteristics of polar cap mesospheric gravity waves observed by an all-sky airglow imager at Resolute Bay, Canada, *J. Geophys. Res.*, *114*, A01311, doi:10.1029/2008JA013652.

Suzuki, S., K. Shiokawa, A. Z. Liu, Y. Otsuka, T. Ogawa, and T. Nakamura (2009b), Characteristics of equatorial gravity waves derived from mesospheric airglow imaging observations, *Ann. Geophys.*, *27*, 1625–1629.

Suzuki, S., T. Nakamura, M. K. Ejiri, M. Tsutsumi, K. Shiokawa, and T. D. Kawahara (2010), Simultaneous airglow, lidar, and radar measurements of mesospheric gravity waves over Japan, *J. Geophys. Res.*, *115*, D24113, doi:10.1029/2010JD014674.

Suzuki, S., F.-J. Lübken, G. Baumgarten, N. Kaifler, R. Eixmann, B. P. Williams, and T. Nakamura (2013a), Vertical propagation of a mesoscale gravity wave from the lower to the upper atmosphere, *J. Atmos. Sol. Terr. Phys.*, *97*, 29–36.

Suzuki, S., K. Shiokawa, Y. Otsuka, S. Kawamura, and Y. Murayama (2013b), Evidence of gravity wave ducting in the mesopause region from airglow network observations, *Geophys. Res. Lett.*, *40*, 601–605, doi:10.1029/2012GL054605.

Tang, J., G. R. Swenson, A. Z. Liu, and F. Kamalabadi (2005), Observational investigations of gravity wave momentum flux with spectroscopic imaging, *J. Geophys. Res.*, *110*, D09S09, doi:10.1029/2004JD004778.

Taylor, M. J., and M. A. Hapgood (1988), Identification of a thunderstorm as a source of short period gravity waves in the upper atmospheric nightglow emissions, *Planet. Space Sci.*, *36*, 975–985.

Vadas, S. L., J. Yue, C.-Y. She, P. A. Stamus, and A. Z. Liu (2009), A model study of the effects of winds on concentric rings of gravity waves from a convective plume near Fort Collins on 11 May 2004, *J. Geophys. Res.*, *114*, D06103, doi:10.1029/2008JD010753.

Vadas, S., J. Yue, and T. Nakamura (2012), Mesospheric concentric gravity waves generated by multiple convective storms over the North American Great Plain, *J. Geophys. Res.*, *117*, D07113, doi:10.1029/2011JD017025.

Vargas, F., G. Swenson, A. Liu, and D. Gobbi (2007), $O(^1S)$, OH, and $O_2(b)$ airglow layer perturbations due to AGWs and their implied effects on the atmosphere, *J. Geophys. Res.*, *112*, D14102, doi:10.1029/2006JD007642.

Wrasse, C. M., et al. (2006), Reverse ray tracing of the mesospheric gravity waves observed at 23°S (Brazil) and 7°S (Indonesia) in airglow imagers, *J. Atmos. Sol. Terr. Phys.*, *68*, 163–181.

Yue, J., S. L. Vadas, C.-Y. She, T. Nakamura, S. C. Reising, H.-L. Liu, P. Stamus, D. A. Krueger, W. Lyons, and T. Li (2009), Concentric gravity waves in the mesosphere generated by deep convective plumes in the lower atmosphere near Fort Collins, Colorado, *J. Geophys. Res.*, *114*, D06104, doi:10.1029/2008JD011244.